1521-0111/86/1/52–61$25.00
MOLECULAR PHARMACOLOGY
Copyright © 2014 by The American Society for Pharmacology and Experimental Therapeutics
http://dx.doi.org/10.1124/mol.114.092098
Mol Pharmacol 86:52–61, July 2014

Desensitization of Functional μ-Opioid Receptors Increases Agonist Off-Rate

John T. Williams

Vollum Institute, Oregon Health and Science University, Portland, Oregon

Received February 4, 2014; accepted April 17, 2014

ABSTRACT

Desensitization of μ-opioid receptors (MORs) develops over 5–15 minutes after the application of some, but not all, opioid agonists and lasts for tens of minutes after agonist removal. The decrease in function is receptor selective (homologous) and could result from 1) a reduction in receptor number or 2) a decrease in receptor coupling. The present investigation used photolysis of two caged opioid ligands to examine the kinetics of MOR-induced potassium conductance before and after MOR desensitization. Photolysis of a caged antagonist, carboxynitroveratryl-naloxone (caged naloxone), blocked the current induced by a series of agonists, and the time constant of decline was significantly decreased after desensitization. The increase in the rate of current decay was not observed after partial blockade of receptors with the irreversible antagonist, β-chlornaltrexamine (β-CNA). The time constant of current decay after desensitization was never more rapid than 1 second, suggesting an increased agonist off-rate rather than an increase in the rate of channel closure downstream of the receptor. The rate of G protein–coupled K^+ channel (GIRK) current activation was examined using photolysis of a caged agonist, carboxynitrobenzyl-tyrosine-[Leu^5]-enkephalin. After acute desensitization or partial irreversible block of MORs with β-CNA, there was an increase in the time it took to reach a peak current. The decrease in the rate of agonist-induced GIRK conductance was receptor selective and dependent on receptor number. The results indicate that opioid receptor desensitization reduced the number of functional receptor and that the remaining active receptors have a reduced agonist affinity.

Introduction

Numerous studies have examined the reduction in μ-opioid receptor (MOR) signaling (desensitization) after the application of a saturating concentration of opioid agonists (Williams et al., 2013). Desensitization is homologous and recovers over a period of 30–60 minutes. One consistent observation is that the extent of desensitization is never complete. There are two potential reasons for the inability to observe a complete block of signaling. One is that some receptors may escape or recover very quickly from desensitization, and the second is that desensitized receptors remain functional but with reduced efficiency. Given the complexity of the downstream signaling events mediated by G protein–coupled receptors, multiple mechanisms could underlie the decline in functional measures (Williams et al., 2013). It therefore is necessary to examine the agonist/receptor interaction more directly before and after desensitization.

A previous study reported that agonist/receptor affinity was increased in living human embryonic kidney (HEK) 293 cells expressing FLAG-MORs after treatment (2 minutes to 2 hours) with saturating concentrations of some, but not all, opioids (Birdsong et al., 2013). The increase in agonist affinity was measured as a decrease in agonist off-rate (K-off) by directly observing the dissociation of a fluorescently labeled peptide agonist. The decrease in K-off was resistant to pertussis toxin treatment and persisted in mouse embryonic fibroblast cells from arrestin knockout animals. Thus, persistent agonist occupation induced a long-lasting state of the receptor having high affinity for agonist. This state was not dependent on downstream signaling, partially recovered over a period of 45 minutes after the removal of agonist, and was interpreted to be the desensitized receptor. However, these experiments did not measure receptor activity. If the desensitized high-affinity receptors were functional, although less efficient, it should be possible to measure a change in ligand-receptor interaction kinetics using a functional assay.

To study the agonist/receptor interaction after desensitization directly in neurons, the present study examined the kinetics of MOR-induced activation and inactivation of potassium conductance in locus ceruleus (LC) neurons in brain slices. The experiments used two caged opioids, carboxynitroveratryl-naloxone (CNV-NLX) and caged carboxynitrobenzyl-tyrosine-[Leu^5]-enkephalin (CYLE). Both caged compounds have little or no affinity for the opioid receptor and can be applied at a high

This work was funded by the National Institutes of Health National Institute on Drug Abuse [Grant R01-DA08163].
dx.doi.org/10.1124/mol.114.092098.

ABBREVIATIONS: BAPTA, 1,2-bis(2-aminophenoxy)ethane-*N*,*N*,*N*′,*N*′-tetraacetic acid; β-CNA, β-chlornaltrexamine; CNV-NLX, carboxynitroveratryl-naloxone; CYLE, carboxynitrobenzyl-tyrosine-[Leu^5]-enkephalin; DAMGO, [D-Ala^2, N-MePhe^4, Gly-ol]-enkephalin; DERM, dermorphin; GIRK channel, G protein–coupled K^+ channel; HEK, human embryonic kidney; MK801, (5*S*,10*R*)-(+)-5-methyl-10,11-dihydro-5*H*-dibenzo[a,d] cyclohepten-5,10-imine; K-off, agonist off-rate; LC, locus ceruleus; ME, [Met^5]-enkephalin; MOR, μ-opioid receptor; NLX, naloxone; OFQ, nociceptin; RGS, regulators of G protein signaling; SST, somatostatin; UFP101, [Nphe^1,Arg^{14},Lys^{15}]nociceptin-NH_2; UK14304, 5-bromo-*N*-(2-imidazolin-2-yl)-6-quinoxalinamine, 5-bromo-*N*-(4,5-dihydro-1*H*-imidazol-2-yl)-6-quinoxalinamine.

concentration for a prolonged period without affecting the opioid receptor. Photolysis results in near instantaneous release of naloxone or [Leu]^5-enkephalin, which then bind to MOR (Banghart and Sabatini, 2012). Naloxone competes with agonist at the receptor to inhibit the receptor-dependent activation of potassium conductance (Banghart et al., 2013). The rate of inhibition is dependent on agonist affinity and concentration, the concentration of CNV-NLX, and the time and intensity of light used for photolysis. Thus, at subsaturating concentrations, the decrease in opioid receptor–dependent potassium conductance can be a reliable measure of the K-off (Banghart et al., 2013). The K-off of agonists from MORs in LC neurons was measured before and after desensitization using the photolysis of CNV-NLX. The results show that desensitization increased the K-off from functional receptors. Using the same approach, the rate of MOR-induced increase in potassium conductance was measured using the caged agonist CYLE before and after desensitization (Banghart and Sabatini, 2012). Desensitization and prior treatment with β-chlornaltrexamine (β-CNA) decreased the activation rate of potassium conductance, suggesting that the kinetics of channel activation were dependent on receptor number. These results indicate that desensitization produced a population of functionally active receptors with apparent low affinity for agonist, which stands in contrast to the observations using fluorescent agonist (Birdsong et al., 2013). Thus, desensitization results in at least two distinct pools of receptor: one functionally active with an apparent low affinity and one nonfunctional with high affinity.

Materials and Methods

Slice Preparation. Horizontal brain slices containing LC neurons were prepared as described previously (Williams and North, 1984). Briefly, rats were euthanized, and the brain was removed, blocked, and mounted in a vibratome chamber (Leica VT 1200S; Buffalo Grove, IL). Horizontal slices (240 μm) were prepared in cold cutting solution containing (in mM): 126 NaCl, 2.5 KCl, 1.2 $MgCl_2$, 2.6 $CaCl_2$, 1.2 NaH_2PO_4, 11 D-glucose and 21.4 $NaHCO_3$, and 0.01 MK801 [(5*S*,10*R*)-(+)-5-methyl-10,11-dihydro-5*H*-dibenzo[a,d]cyclohepten-5,10-imine; Abcam, Cambridge, UK], equilibrated with 95% O_2/5% CO_2. Slices were stored at 34°C in glass vials with oxygenated (95% O_2/ 5% CO_2) artificial cerebrospinal fluid containing (in mM): 126 NaCl, 2.5 KCl, 1.2 $MgCl_2$, 2.6 $CaCl_2$, 1.2 NaH_2PO_4, 11 D-glucose, and 21.4 $NaHCO_3$.

Recording. After an incubation period of 30 to 60 minutes, slices were hemisected and transferred to the recording chamber and superfused with 34°C artificial cerebrospinal fluid at a rate of 1.5 ml/minute. Whole-cell recordings were made with an Axopatch 1D amplifier (Molecular Devices, Sunnyvale, CA) in voltage-clamp mode (V_{hold} = −60 mV). Recording pipettes (1.7–2.1 MΩ) were filled with internal solution containing (in mM): 115 potassium methanesulfonate or potassium methyl sulfate, 20 NaCl, 1.5 $MgCl_2$, 5 HEPES(K), 10 BAPTA [1,2-bis (2-aminophenoxy)ethane-*N*,*N*,*N*′,*N*′-tetraacetic acid] or 0.1 EGTA, 2 Mg-ATP, 0.2 Na-GTP, pH 7.4, 275-280 mOsM. Series resistance was monitored without compensation and was <15 MΩ. Current was continuously recorded at 200 Hz with PowerLab (chart version 5.4.2; AD Instruments, Colorado Springs, CO). Episodic currents were recorded at 10 kHz for 1 minute using AxoGraphX (1.4.3; AxographX, Berkeley, CA). Drugs were applied by bath superfusion.

Uncaging of CNV-NLX was carried out with full-field illumination using a 405-nm LED (Thorlabs, Sterling, VA) coupled through a 60× objective (Olympus 0.9 numerical aperture). Light power was 10 mW at the back aperture of the objective. A solution containing CNV-NLX (5 μM, in 6 ml) was recirculated for at least 5 minutes before an uncaging experiment. Opioid agonists were added to the solution containing CNV-NLX before photolysis. In most experiments, slices were exposed to only a single light flash. In all experiments, a saturating concentration of the α_2-adrenoceptor agonist UK14304 [5-bromo-*N*-(2-imidazolin-2-yl)-6-quinoxalinamine, 5-bromo-*N*-(4,5-dihydro-1*H*-imidazol-2-yl)-6-quinoxalinamine; 3 μM] was applied, and the resulting current was used as a postsynaptic control. In many experiments, the amplitude of opioid-induced current was presented as a fraction of the current induced by UK14304. Uncaging of CYLE (20 μM) was carried out in a recycled solution with full-field illumination using a 365-nm LED (Thorlabs) coupled through a 60× objective (Olympus 0.9 numerical aperture, 1.5 mW at objective). Morphine was obtained from the National Institute on Drug Abuse. [Met]^5-Enkephalin (ME), [D-Ala^2, N-MePhe^4, Gly-ol]-enkephalin (DAMGO), endomorphin-2, and β-CNA were obtained from Sigma-Aldrich (St. Louis, MO). Dermorphin (DERM) was obtained from Phoenix Peptides (Burlingame, CA). Somatostatin (SST) was obtained from Bachem (Bubendorf, Switzerland). Nociceptin (OFQ), UK14304 and idazoxan, and caged noradrenaline were obtained from Tocris Bioscience (Bristol, UK). CNV-NLX prepared by Shanghai Medicilon, Inc. (Shanghai, China), using the procedure described in Banghart et al. (2013). CYLE was obtained from Peptech Inc. (Bedford, MA) and further purified by high-performance liquid chromatography as described in Banghart et al. (2012).

Data Analysis. Summary data are presented as mean ± S.E.M. The time constant of decay was fit to a single exponential using AxoGraphX. The time courses covered the area from at least 5–95% of the total time course of the decline in agonist-induced current. Statistical analysis was carried out using paired or unpaired Mann–Whitney rank sum test where $P < 0.05$ was considered significant.

Results

Increased Rate of Current Decay Induced by Naloxone after Desensitization. CNV-NLX (5 μM) was recirculated for a minimum of 5 minutes before the application of ME. ME induced an outward current that was completely blocked after a flash of light to release naloxone (photolysis of CNV-NLX, 405 nm, 5 seconds) (Fig. 1). The time constant of inhibition was dependent on the concentration of ME. At a saturating concentration (30 μM), the time constant of decay was about 3.5 seconds and at a subsaturating concentration (1 μM) was about 1 second (Fig. 1) (Banghart et al., 2013). The rate of naloxone block of the ME current was expected to be concentration dependent based on the fact that naloxone and ME compete for the same binding site on the receptor. With a prolonged application of ME (30 μM), the current peaked and desensitized over 10 minutes (Fig. 1). The time constant of current decay induced by photolysis of CNV-NLX (5 μM, 5 seconds) after 10 minutes of ME decreased to about 1.5 seconds, roughly the same as the rate of decline measured with a subsaturating concentration of ME (1 μM; Fig. 1). Thus, after desensitization, naloxone competes more effectively with a saturating concentration of ME.

The high-affinity agonist DERM was used previously to characterize the rate of CNV-NLX–induced decay over a wide range of concentrations (Banghart et al., 2013). At low concentrations (<100 nM), the time constant of decay reached a limiting level of about 4 seconds (Banghart et al., 2013). That limiting level was suggested to represent the off-rate of DERM from the receptor. Photolysis of CNV-NLX (5 μM, 5 seconds) at the peak of the outward current induced by DERM (1 μM) blocked the current with a time constant of about 6.5 seconds (Fig. 2). After 10 minutes, the current induced by DERM (1 μM) declined to about 50% of the peak. Photolysis of

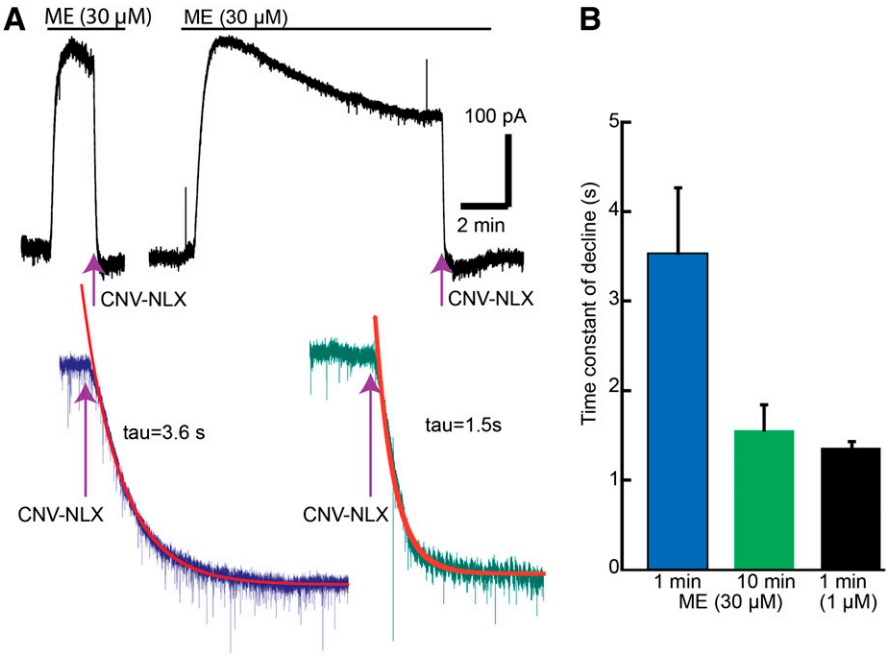

Fig. 1. The rate of current decline induced by photolysis of CNV-NLX (5 μM) increased after desensitization induced by ME (30 μM). (A) Two experiments, one where photolysis of CNV-NLX was applied at the peak of the ME-induced current and the second 10 minutes after the application of ME. Examples of the change in current induced by CNV-NLX at the peak (left) and 10 minutes after the application of ME (right) are shown. (B) Summarized results showing the time constant of decay at the peak (blue), after ME (10 minutes, green), and at the peak of a nonsaturating concentration of ME (1 μM, black).

CNV-NLX blocked the remaining current with a time constant of about 3 seconds (Fig. 2). Although there is considerable spread in the results, the mean value of the time constant of decline was faster than that observed using much lower concentrations of DERM (10–100 nM) (Banghart et al., 2013). The decay, however, remained slower than the maximum rate of decline (1–2 seconds) observed with multiple low-affinity agonists (Banghart et al., 2013).

The increase in the rate of current decay induced by CNV-NLX was not dependent on the continued presence of opioid agonists. Slices were incubated in a saturating concentration of ME (30 μM, 1 to 2 hours) to induce desensitization. After the incubation, the ME was washed (5–15 minutes), and recordings were made. During the recording, CNV-NLX (5 μM, 5 minutes) was equilibrated, followed by application of DERM (1 μM). Once the DERM-induced current reached a peak, photolysis of

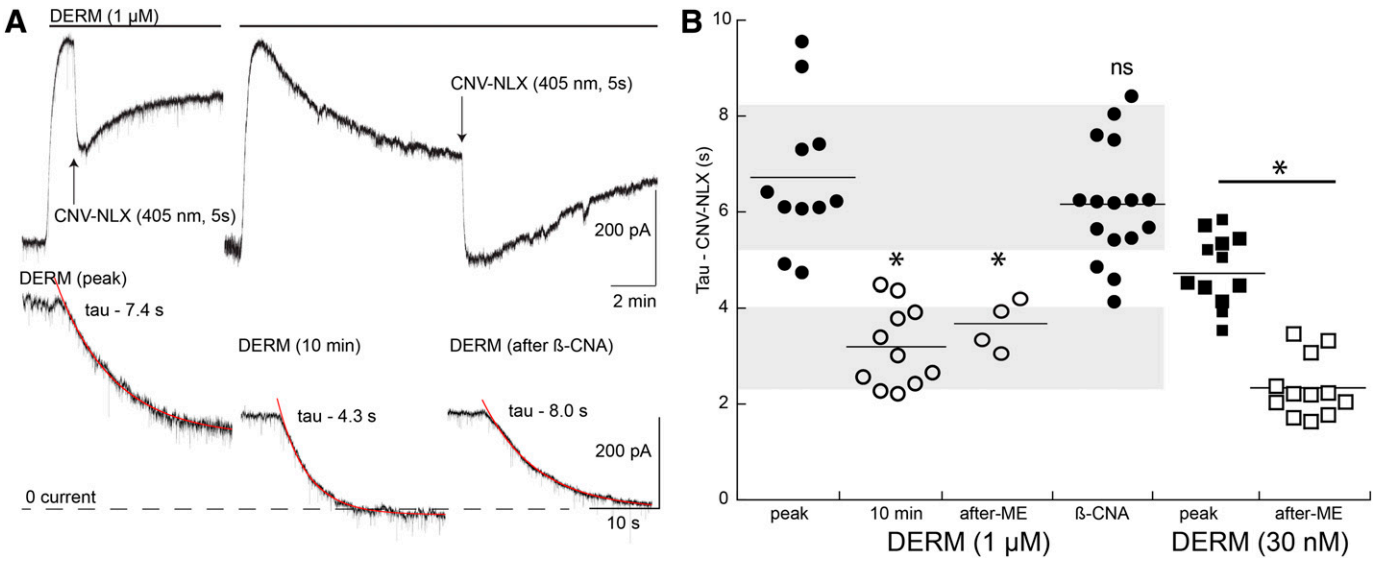

Fig. 2. The rate of current decline increased after desensitization with the high-affinity agonist DERM (1 μM). (A) Two experiments showing the inhibition of the DERM current at the peak of the current (left) and 10 minutes after the application of DERM (right). Example traces of the current decline induced by CNV-NLX at the peak (peak), 10 minutes after DERM (DERM, 10 minutes), and after partial blockade of MORs with β-CNA (after β-CNA) are shown. (B) Dot plot of the time constant of CNV-NLX–induced inactivation of the DERM current at the peak (peak; ●), 10 minutes after DERM (10 minutes; ○), and 5–15 minutes after slices were desensitized with ME (30 μM, 1 to 2 hours, after-ME; ○) and after treatment with β-CNA (post–β-CNA; ●). Shaded areas illustrate the standard area of the time constant of decay measured at the peak (top) and after 10 minutes (bottom). Closed squares indicate the time constant of current decay induced by CNV-NLX after the application of DERM (30 nM). Larger squares are from the current experiments, and smaller squares are from published work. Open squares are the time constant of current decay induced by CNV-NLX in slices that were predesensitized by incubation with ME (30 μM, 30–90 minutes and washed before application of CNV-NLX, after ME). *$P < 0.05$ by unpaired Wilcoxon–Mann–Whitney rank sum test.

CNV-NLX blocked the outward current with a time constant of about 4 seconds, the same as that found after acute desensitization (Fig. 2B). Thus, the induction of desensitization with ME resulted in an increase in the rate of current decline that outlasted the presence of agonist.

The increase in the rate of naloxone-induced decline in current suggested that the agonist affinity decreased after desensitization; however, after photolysis of CNV-NLX in the high concentration of DERM (1 μM), the outward current began to recover. This recovery was presumably the result of naloxone dissociation and rebinding of DERM. To obtain a more quantitative assessment of a change in agonist affinity, a low concentration of DERM (30 nM) was used. This concentration of DERM was previously shown to be low enough that there was no detectable rebinding of agonist within the time course of the experiment. Thus, the decline in current induced by CNV-NLX under these conditions is thought to be dependent on the K-off of DERM. The CNV-NLX–induced decline in the current in the presence of DERM (30 nM) was measured in untreated slices and slices that were incubated in ME (30 μM, 30–120 minutes) and washed for 10–20 minutes before the application of DERM (30 nM). In previous experiments, the time constant of decline induced by CNV-NLX in the presence of DERM (30 nM) was 4.8 ± 0.43 seconds (n = 5; Banghart et al., 2013). This value was reproduced in additional current control experiments (4.9 ± 0.23 seconds, n = 7), so the two sets of data were combined (4.8 ± 0.21 seconds, n = 12). In slices that were incubated in ME (30 μM, desensitized), the CNV-NLX–induced decline in the DERM-induced (30 nM) current was significantly faster (2.38 ± 0.18 seconds, n = 12, $P < 0.05$; Fig. 2B). These values, along with the determination of the agonist on-rate for a fluorescent DERM (DERM-A594, $6.12 \cdot 10^5\ M^{-1}s^{-1}$ (Birdsong et al., 2013), were used to estimate the increase in Kd that resulted from desensitization (control 340 nM, desensitized 687 nM). Thus, the results suggest that desensitization reduced the affinity of DERM for the receptor by about 50%.

No Change in the Rate of Naloxone Block after Reduction of Functional MORs with β-CNA. It is possible that the decline in the amplitude of the current induced by desensitization with DERM could affect the rate of blockade by CNV-NLX. This possibility was examined using the partial irreversible inactivation of MORs with β-CNA (100 nM, 2 minutes). This treatment decreased the current induced by DERM (1 μM, normalized to the current induced by a saturating concentration of UK14304, 3 μM) to a similar extent as that observed following desensitization (DERM/UK14304; peak 1.27 ± 0.05, n = 11; desensitized 0.66 ± 0.4, n = 10; post–β-CNA 0.63±0.06, n = 16). The time constant of inactivation was not, however, significantly changed from that found at the peak of the DERM current (Fig. 2). The results indicate that the simple removal of receptors using β-CNA did not affect the rate of receptor blockade after photolysis of CNV-NLX, unlike what was observed after acute desensitization. Thus, the increase in the rate of current decay by photolysis of CNV-NLX after desensitization resulted from a decrease in agonist-dependent signaling. The increase in deactivation rate observed with both ME and DERM is most readily interpreted as an increase in K-off, which suggests that desensitization decreased agonist affinity.

Increased Rate of Naloxone Current Decay Is Receptor-Selective. It is possible that the increase in the rate of decline caused by naloxone results from a change that is independent of MOR. Experiments were carried out with the use of saturating concentrations of SST (3 μM) and OFQ (3 μM) applied for 10 minutes, both of which also activate G protein–coupled K^+ channel (GIRK) channels in LC neurons. Both agonists resulted in a peak and decline in the outward current that was similar to that seen with a saturating concentration of DERM (Virk et al., 2009; Llorente et al., 2012). During the application of either SST (3 μM) or OFQ (3 μM), CNV-NLX (5 μM, 5 minutes) was equilibrated in the recycling solution and DERM (1 μM) was applied in the continued presence of SST or OFQ. DERM increased the outward current, and photolysis of the CNV-NLX resulted in an inhibition of the current. In the presence of SST, the time course of the inhibition was not different from the acute application of DERM alone (Fig. 3). Treatment with OFQ resulted in a small increase in the rate of decay induced by CNV-NLX (Fig. 3). To investigate more fully the potential interaction between OFQ and DERM, slices were incubated in OFQ (3 μM) for periods of 30–90 minutes, OFQ was washed,

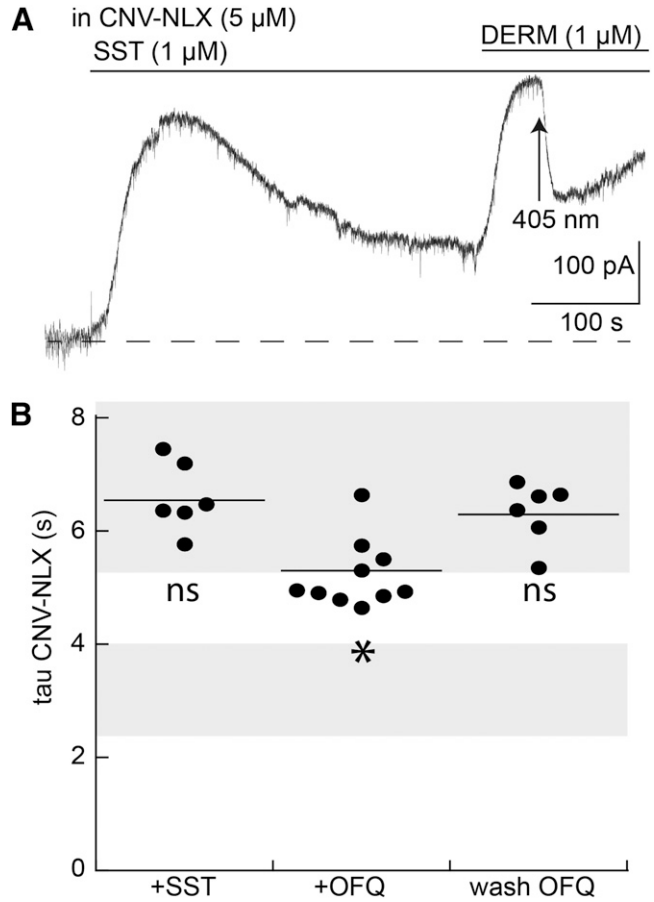

Fig. 3. Application of DERM (1 μM) after desensitization with SST and OFQ does not change the rate of current decline induced by CNV-NLX. (A) Example trace of an experiment in which the current induced by SST (1 μM, 10 minutes) peaked and decayed, followed by the application of DERM and photolysis of CNV-NLX. (B) Dot plot of experiments measuring the time constant of current decay induced by CNV-NLX at the peak of the current induced by DERM (1 μM) in the presence of somatostatin (DERM + SST), OFQ (DERM + OFQ) and after the washout of OFQ (DERM wash OFQ). Shaded areas are the same as in Fig. 2, illustrating the standard error of experiments with DERM alone at the peak (top) and after 10 minutes (bottom). *$P < 0.05$ by one-way ANOVA compared with DERM alone; Dunnett post hoc. ns, not significant.

and the OFQ antagonist, UFP101 ([Nphe^1,Arg^{14},Lys^{15}]nociceptin-NH_2; 3 μM), was applied before the addition of DERM (1 μM). In the absence of a current induced by OFQ, the rate of naloxone block of the current induced by DERM was not different from that of control (Fig. 3). The small effect of OFQ on the inactivation of the current induced by DERM when applied simultaneously may suggest a common component of downstream signaling. However, this component was small and reversed rapidly on blockade of the OFQ receptor. Thus, the increase in the rate of current decay was homologous resulting from the selective activation of MOR.

Increase in Rate of Naloxone Block Depends on Agonist Affinity. The relative role of agonist affinity on the increased rate of receptor blockade by CNV-NLX was examined using a series of agonists with different affinity for the receptor (Banghart et al., 2013). With the exception of morphine, application of each agonist for 10 minutes resulted in a decline from the peak current. Previous work found that the most reliable way to induce desensitization with morphine was to treat animals for 6 to 7 days with morphine (Levitt and Williams, 2012). Desensitization (and tolerance) to morphine was induced by the chronic treatment of animals with morphine using osmotic minipumps; slices were cut and maintained in morphine (1 μM) (Levitt and Williams 2012). The current induced by CNV-NLX from morphine-treated animals was compared with that induced in slices taken from untreated animals, where the slices were cut and maintained in morphine.

The amplitude of the current and the rate of current decline induced by CNV-NLX were measured for a series of agonists before and after desensitization. To induce desensitization, it was necessary to use a saturating concentration of each agonist. The amplitude of the opioid-induced current in each experiment was normalized to the current induced by a saturating concentration of the α_2-adrenoceptor agonist, UK14304 (3 μM; Fig. 4B). After desensitization with each agonist (DERM, endomorphin-2, DAMGO, ME, and morphine), there was a significant decrease in the amplitude of the opioid current and a decrease in the time constant of current decline induced by CNV-NLX (Fig. 4A). The decrease in time constant after desensitization varied with the agonist. In the case of high-affinity agonists, DERM, and endomorphin-2, the rate of decline decreased to about 3 to 4 seconds. As indicated previously, the rate of decline in experiments using high concentrations of agonist represents the combination of the affinity of the agonist and competition between agonist and naloxone for the receptor (Banghart et al., 2013). In the case of DERM and endomorphin-2, the rate of decline is significantly longer than the rate of decline induced by nonsaturating concentrations of lower-affinity agonists (Fig. 4A; 1.5 seconds). After desensitization using lower-affinity agonists, particularly morphine, the increase in the rate of decline was smaller and not significantly different from the rate of decline induced by subsaturating concentrations of low-affinity agonists (Fig. 4A, horizontal line). This value is most likely limited by the decline in second-messenger signaling (Ingram et al., 1997; Banghart et al., 2013). Given the similarity in this limiting time constant obtained with the use of low concentrations of agonists, it is likely that desensitization decreased agonist affinity but not the rate of decline in intrinsic signaling that follows activation of the receptor.

Desensitization Decreased Agonist-Induced Current and Rate of Activation. The decrease in the steady-state amplitude of the opioid-induced current after desensitization is well established; however, the kinetics of current activation has not been tested. Photolysis of the caged opioid agonist CYLE was used to examine the amplitude and rising phase of agonist-induced current before and after acute desensitization (Fig. 5). CYLE (20 μM) was recycled in the presence of bestatin (10 μM) and thiorphan (1 μM) to block peptidase activity, and photolysis was induced using an LED light source (100 milliseconds, 365 nm). Flashes were applied at 3-minute intervals, and the amplitude (150–400 p*A*) and kinetics (rise time 160 milliseconds; time to peak = 0.6–1.2 seconds) of the current remained constant for at least 30 minutes using this protocol.

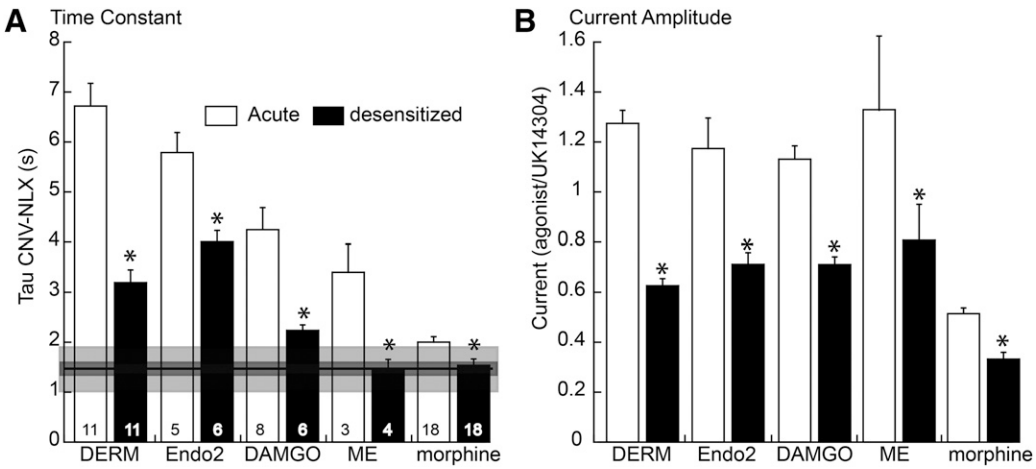

Fig. 4. Summary of the results obtained for five agonists showing the increase in the rate of decline after desensitization. (A) Histogram of the time constant of current decay-induced photolysis of CNV-NLX (5 μM) for DERM (1 μM, same data as in Fig. 2), endomorphin-2 (Endo2; 1 μM), DAMGO (1 μM), ME (30 μM, same data as in Fig. 1), and morphine (1 μM). (Open bars) Measured at the peak current; solid bars are 10 minutes after application of the agonist, with the exception of morphine, which was after treatment of the animal for a week. In each case, the increase in the rate of decline after prolonged treatment (black bars) was significantly different from that measured at the peak. Horizontal line and dark and light gray boxes are the mean, S.E.M., and S.D. of the time constant of decline in the current induced by EC_{50} concentrations of low-affinity agonists (codiene, DAMGO, ME, DSLET, oxycodone, and morphine, taken from Banghart et al., 2013). (B) Histogram of current amplitude before and after desensitization with the indicated agonist (normalized to the current induced by UK14304, 3 μM). $^*P < 0.05$ by unpaired Wilcoxon–Mann–Whitney rank sum test.

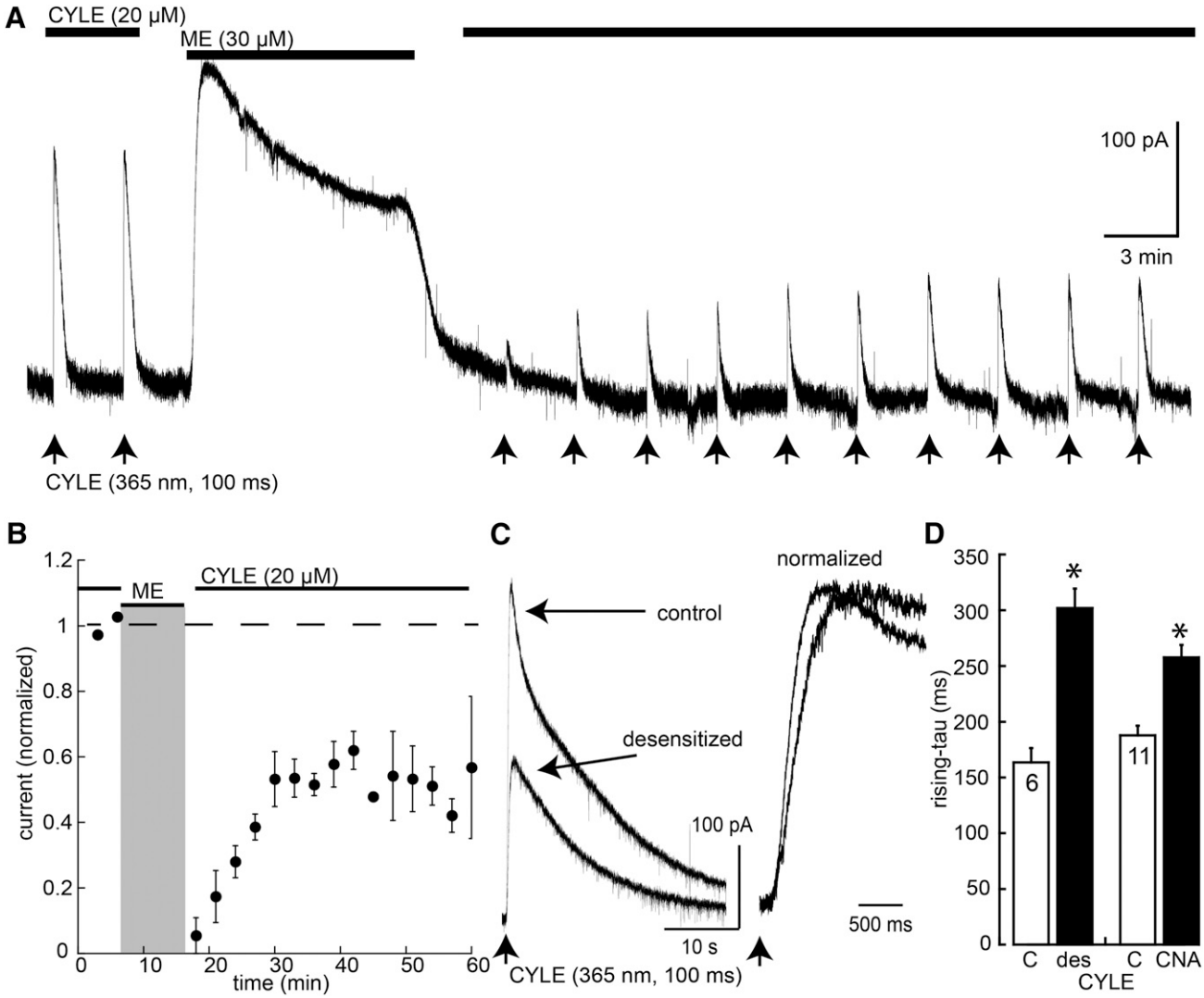

Fig. 5. Desensitization decreased the amplitude and rate of rise of the current induced by photolysis of CYLE. (A) Example trace of an experiment where the current induced by CYLE is shown before and after desensitization with ME (30 μM). Arrows indicate the light flash. (B) Summarized results showing the inhibition and recovery of the amplitude of the current induced by CYLE. (C) Two superimposed traces of the current induced by CYLE before and after recovery from desensitization (10–20 minutes). (D) Summarized results showing the increase in the rise (time constant) before (C) and after recovery from desensitization (des) and before (C) or after application of β-CNA (CNA; 100 nM, 2 minutes). *$P < 0.05$ by paired Wilcoxon–Mann–Whitney rank sum test.

After two or three light flashes, the CYLE-containing solution was washed out, and ME (30 μM) was applied for 10 minutes and washed for 5 minutes before the recycling CYLE again. The initial amplitude of current induced by photolysis after desensitization was dramatically reduced and partially recovered over a period of 15 to 20 minutes (Fig. 5). The rate of rise and time to reach the peak current were consistently slowed after desensitization (Fig. 5). The decrease in the amplitude of current amplitude after desensitization was expected, although recovery from desensitization was less than that observed in previous experiments using steady-state application of agonist (Osborne and Williams, 1995; Fiorillo and Williams, 1996; Quillinan et al., 2011).

The rate of current rise to a steady state was examined using a prolonged flash (5 seconds, CYLE 20 μM + bestatin 1 μM + thiorphan 10 μM). The first flash resulted in the activation of current with a time constant of 241 ± 26 milliseconds (n = 6). In every case, the current peaked and started to decline during the 5-second exposure to light (Fig. 6). The current declined to the baseline after 2 to 3 minutes. A second flash resulted in a smaller current, and the rate of rise was slowed (426 ± 68 milliseconds) with the early component of the current being the most affected. A third flash resulted in a smaller and more slowly rising current (473 ± 85 milliseconds). The decrease in amplitude and rate of rise after the first flash was taken as a sign of acute desensitization. Finally, slices were incubated in ME (30 μM, 30–90 minutes) and washed for 10–15 minutes before applying a 5-second flash (CYLE, 20 μM). In these experiments, the time constant of current rise was increased to 651 ± 76 milliseconds (n = 6, Fig. 6C). Thus, similar to short flashes, prior desensitization decreased the rate of current rise induced by a flash long enough to allow the current to reach a steady state.

Treatment with β-CNA Decreased the Rate of Agonist-Induced Current. The small decrease in the rate of current activation after desensitization could potentially result from

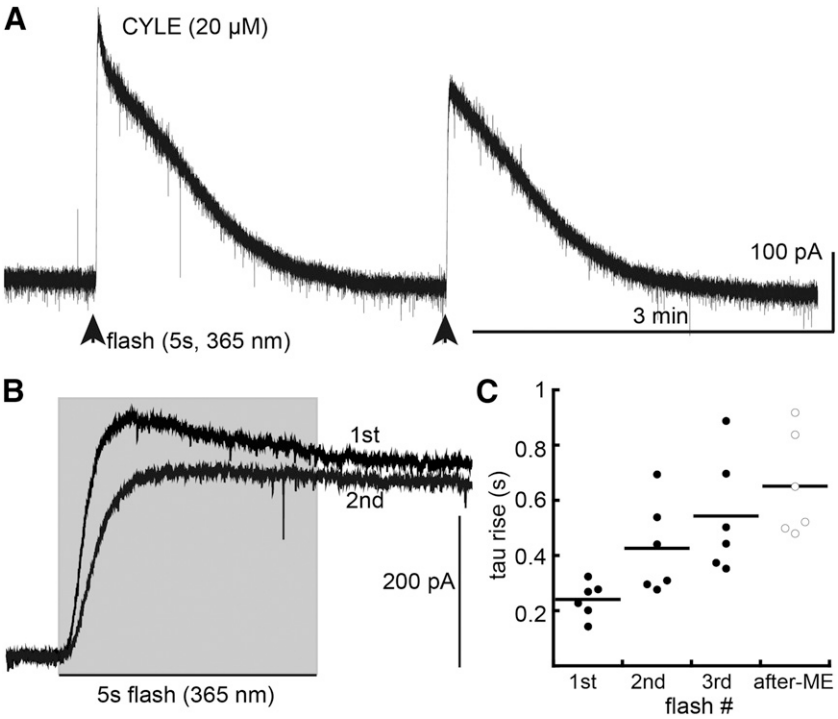

Fig. 6. Repeated long flashes decreased amplitude and rate of current rise induced by photolysis of CYLE. (A) Example trace of an experiment showing the current induced by two 5-second flashes of CYLE. (B) Two superimposed traces showing the change in rate of rise of current induced by two flashes of CYLE. (C) Summarized results showing the time constant of current activation induced by CYLE on three separate flashes applied at 3- to 5-minute intervals (closed circles). Open circles summarize experiments where slices were incubated in ME (30 μM, 30–90 minutes) to induce desensitization and washed before photolysis of CYLE (20 μM, 5 seconds, after ME).

a change in affinity of [Leu]^5-enkephalin for the receptor or a change in downstream signaling. Given the change in the amplitude of current induced by CYLE, experiments were done after treatment of the slice with β-CNA to remove receptor reserve. The rising phase of the current induced by CYLE was examined before and after treatment of slices with β-CNA (100 nM, 2 minutes, followed by a 10- to 15-minute wash). The amplitude of the current induced by CYLE after treatment of the slice with β-CNA was decreased by about 50%, the same as that following desensitization (CYLE control 232 $\pm$ 25 pA, desensitized 103 $\pm$ 13 pA, $n = 14$; β-CNA control 214 $\pm$ 25 pA, post–β-CNA 96 $\pm$ 14, $n = 11$). Likewise, the rate of rise of the current decreased after treatment with β-CNA (Fig. 5D). Thus, removal of functional receptors with β-CNA resulted in the same change in the rising phase of the CYLE-induced current as that after desensitization with a saturating concentration of ME. This suggests that there are two components involved in desensitization. One is a decrease in the apparent affinity of functional receptors for agonists measured as an increase in deactivation rate with photolysis of CNV-NLX. The second is a reduction in the number of functional receptors measured as a change in activation rate with CYLE.

A Heterologous Mechanism Does Not Alter MOR Activation Kinetics. Both SST and OFQ receptors have been shown to desensitize readily (Fiorillo and Williams, 1996; Virk et al., 2009). Activation of MORs with CYLE was examined before and during the application of saturating concentrations of OFQ (3 μM, 10 minutes). Although the amplitude of the current induced by CYLE was decreased by occlusion, the time constant of the rise in current induced by CYLE was not changed (Fig. 7). Thus, desensitization of non-opioid receptors did not affect the rate at which the activation of MORs activated potassium current.

The amplitude and rate of current activation induced by CYLE were also examined before and during the application of morphine (1 μM; Fig. 7). This concentration results in a current

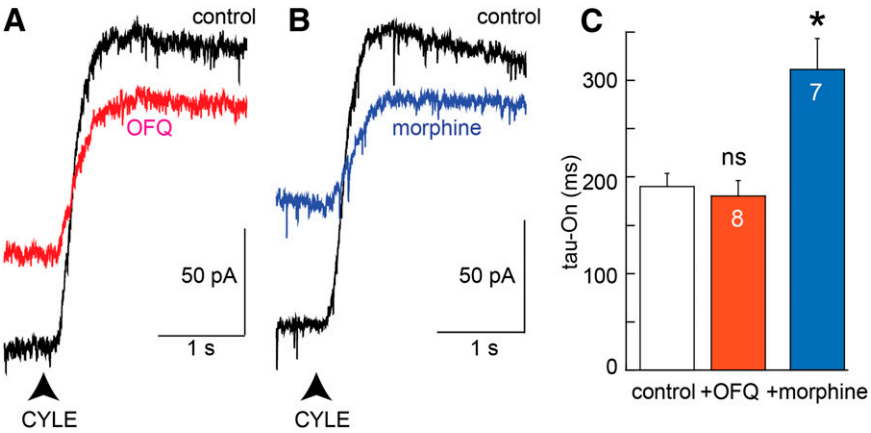

Fig. 7. CYLE-induced current is decreased by a receptor selective mechanism. (A) Example traces of the current induced by CYLE before (black) and after desensitization with OFQ (1 μM, 8–10 minutes, red). (B) Example traces of the current induced by CYLE (black) and in the presence of morphine (1 μM, 8–10 minutes, blue). (C) Summarized results measuring the time constant of the rate of rise. Experiments with OFQ and morphine were paired, and the control tau-On were combined for illustration. Statistics were done with a paired Wilcoxon–Mann–Whitney rank sum test (*$P < 0.05$). ns, not significant.

that is about 75% of the peak such that the amplitude of the current induced by CYLE was reduced by competition for MOR (Levitt and Williams, 2012). In these experiments, the rate of rise of the current induced by CYLE was also decreased (Fig. 7). Thus, the occupation of receptors with morphine, a partial agonist, reduced the rate of current activation similar to that observed after desensitization or treatment with β-CNA.

To determine whether the increase in rise time of the current induced by CYLE resulted from a change in downstream signaling, the rise time of the current induced by photolysis of caged noradrenaline was examined before and after desensitization induced by ME (30 μM, 10 minutes). Caged noradrenline (100 μM) was recycled, and repeated flashes (365 nm, 100 milliseconds, 1-minute intervals) were applied to activate α_2-adrenoceptors (Fig. 8). This protocol resulted in reproducible outward currents with a time to reach the peak of approximately 500 milliseconds. The current was increased by cocaine (10 μM) and was blocked by the α_2-adrenoceptor antagonist idazoxan (1 μM). The current induced by photolysis of caged noradrenaline was initially occluded after the addition of DERM (10 μM, 10 minutes). As the DERM-induced current declined, the current induced by caged noradrenaline increased (Fig. 8). After the addition of naloxone (1 μM), the current induced by caged noradrenaline increased to 90% of the initial amplitude. The time it took to reach the peak current induced by noradrenaline was not changed during or after the application of DERM. Thus, desensitization of MOR did not affect the signaling induced by activation of the α_2-adrenoceptor.

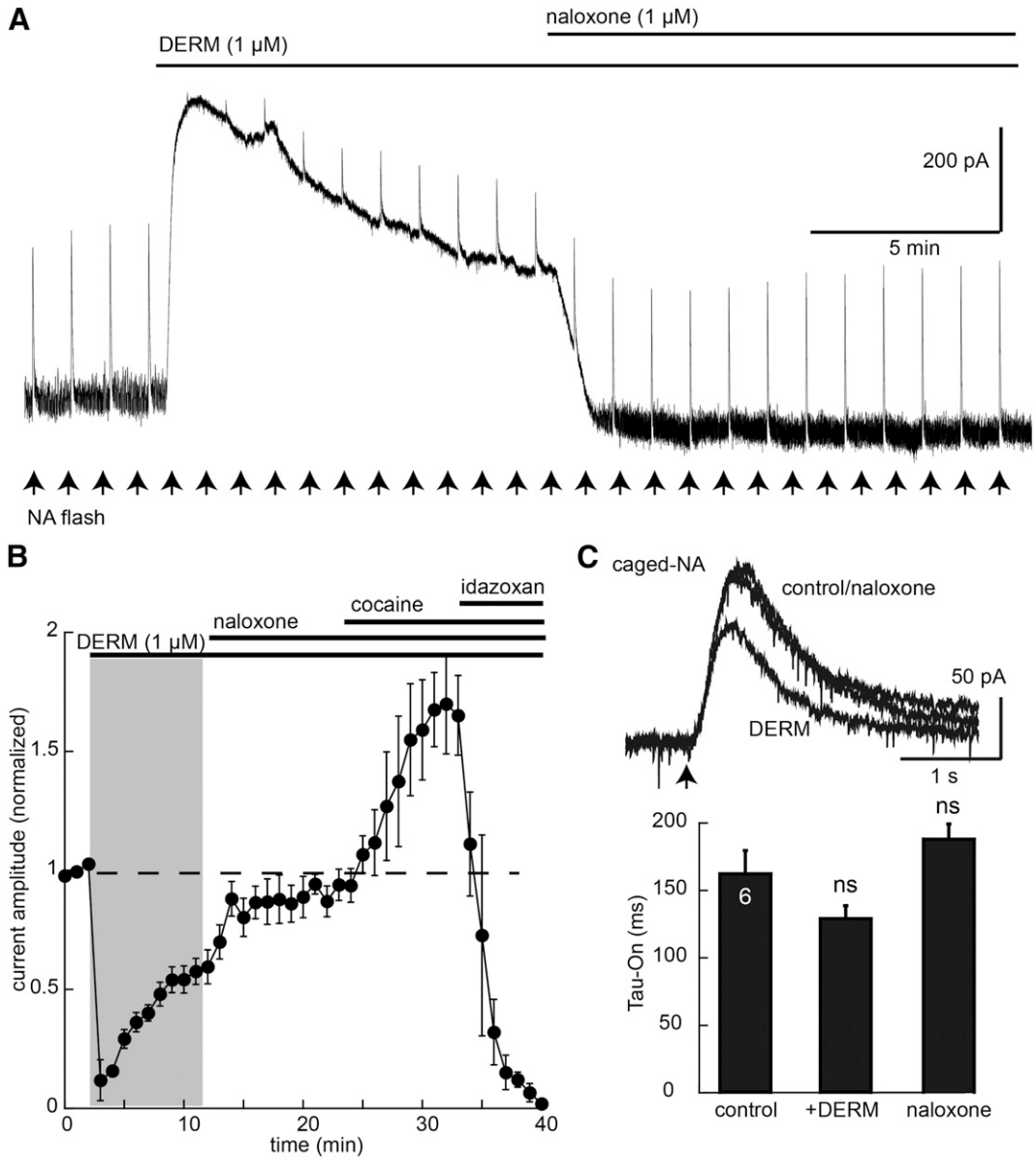

Fig. 8. MOR desensitization does not change the noradrenaline activation of GIRK. (A) Example trace showing the current induced by photolysis of noradrenaline (arrows) during the application of DERM (1 μM) and DERM + naloxone (1 μM). (B) Summarized results showing the NA current decreased in DERM through occlusion, the reversal with naloxone (1 μM), the increase induced by cocaine (10 μM), followed by the inhibition with idazoxan (1 μM). (C) Superimposed traces of the current induced by caged noradrenaline (NA) before, 7–10 minutes in DERM, and after reversal with naloxone (1 μM). At bottom is the summarized rate of rise of the noradrenaline-induced current. Statistics tested with an analysis of variance, Dunnett's post hoc test.

Discussion

With the use of caged opioids, two distinct changes in opioid receptor signaling were observed after desensitization of MORs in LC neurons. First, there was an increase in the rate at which rapid application of naloxone decreased MOR-dependent potassium current. Second, the rate of potassium current activation induced by photolysis of caged agonist was decreased after desensitization. There is a distinct mechanistic difference between the two observations. The increase in the rate of current inactivation induced by CNV-NLX was not dependent on the receptor number. Reducing receptor number with an irreversible antagonist did not change the rate of current inhibition induced by CNV-NLX. The decrease in the rate of current activation induced by CYLE was, however, dependent on the number of receptors. Thus, opioid receptor desensitization results in two distinct changes in receptor-dependent kinetics: a reduction in the number of active receptors measured with the caged agonist and a decrease in agonist/receptor affinity of the remaining functional receptors measured with CNV-NLX. These functional receptors are distinct from the high-affinity, most likely nonfunctional, receptors that were observed in HEK cells after desensitization using a fluorescent binding assay (Birdsong et al., 2013).

Measuring Agonist Off-Rate with a Functional Assay. The decline in potassium current induced by the photolysis of CNV-NLX is dependent on the concentration of agonist, the concentration of naloxone released by photolysis, and the K-off of the agonist from the receptor (Banghart et al., 2013). To induce desensitization, it was necessary to apply a saturating concentration of each agonist such that on photolysis naloxone competed with the agonist at the receptor. Although the on rate of naloxone for the receptor is rapid, competition between naloxone and the saturating agonist concentration slowed the rate of current decline (Banghart et al., 2013). The increase in the rate of current decline induced by photolysis of CNV-NLX after desensitization therefore results from a more effective competition of naloxone for MOR. The most obvious explanation for this result is a reduction in the affinity of agonist for MOR. This conclusion is supported by results obtained with a subsaturating concentration of DERM (30 nM). Desensitization decreased the affinity of DERM for the receptor by about 50%.

The limiting rate of decline induced by photolysis of CNV-NLX was 1 to 2 seconds, a value that is thought to represent the maximum rate of GIRK inactivation (Ingram et al., 1997; Banghart et al., 2013). After desensitization, the rate of decline was never less than this limiting value, suggesting that desensitization resulted in a decrease in agonist/receptor affinity rather than an increase in the rate of downstream mechanisms that terminate G protein–dependent signaling.

Pharmacologic studies have indicated that acute desensitization reduces the number of functional receptors by about 90% (Osborne and Williams, 1995). The current that remained after desensitization is therefore dependent on a small population (10%) of receptors that have a lower apparent affinity for agonists. Binding assays on living cells after a desensitization protocol report that most receptors were in a high-affinity state (Birdsong et al., 2013). Although the G protein–coupled receptor is considered to have high affinity for agonists, the high-affinity state that was induced by desensitization in the HEK cells is unlike the canonical model of G protein–coupled receptor/G protein interaction (Werling et al., 1988). The desensitized receptor was insensitive to prior treatment with pertussis toxin (Birdsong et al., 2013). This result was interpreted to indicate that the desensitized (functionally uncoupled) receptor adopted a high-affinity state that was independent of G proteins. There is also precedent that agonist affinity increased with prolonged agonist incubation in hippocampal membranes (Scheibe et al., 1984). Had these high-affinity receptors been functional, the agonist off-rate seen in the present study would be expected to slow several-fold. Previous studies looking at changes in affinity after desensitization and/or tolerance have not differentiated functional from nonfunctional receptors. Therefore, by implementing a functional assay, the results provide evidence for at least two distinct pools of receptors following homologous desensitization: one functionally active with an apparent low affinity and one nonfunctional with high affinity.

Potential Mechanisms. The decrease in functional receptors found after desensitization is largely homologous, although the degree of heterologous desensitization is dependent on the age of the animal (Llorente et al., 2012). The activation of the same potassium conductance through the OFQ and SST receptors had little or no effect on the naloxone-induced inactivation of the current induced by DERM. The decay in the potassium current induced by naloxone was insensitive to the continued presence of a saturating concentration of SST, even after the current induced by SST had declined to about 50% of the peak. Thus, a global increase in the presence of molecules that may increase the inactivation of GIRK, such as regulators of G protein signaling (RGS) proteins, may not account for the results. This, however, does not rule out the potential role of RGS proteins that are selectively associated with MORs.

Potential receptor-selective mechanisms include phosphorylation. In spite of considerable effort, there is no consensus on the role of phosphorylation in acute MOR desensitization, particularly the in brain (Williams et al., 2013). In HEK cells expressing MORs, multiple sites on the C-terminal tail were phosphorylated by morphine and DAMGO (Lau et al., 2011; Just et al., 2013; reviewed in Williams et al., 2013). Mutation of a sequence of phosphorylation sites beginning at S375 to alanines eliminated receptor trafficking and arrestin binding (Lau et al., 2011). Another sequence of C-terminal residues, TSST, starting at T354, was also identified as agonist-dependent phosphorylation sites (Lau et al., 2011). Mutation of those residues to alanine did not change the trafficking of receptors induced by DAMGO. The role of phosphorylation of these amino acids, both STANT (375-380) and TSST (354-357), in acute desensitization particularly in neurons is not known (but see Wang et al., 2002).

Receptor Number Regulates the Rate of Current Activation. A surprising observation was that the decrease in the rate of CYLE-induced current after MOR desensitization was dependent on receptor number. Treatment of slices with the irreversible antagonist β-CNA decreased the rate of potassium current activation induced by CYLE to the same extent as that found after desensitization. The rate of current activation induced by opioids in acutely isolated LC neurons had a time constant of about 700 milliseconds (Ingram et al., 1997). This value is significantly slower than that found in the present study; however, the receptor reserve in acutely isolated neurons was reduced to the point that morphine was ineffective at activating a current. In fact, in the acutely dissociated cells,

morphine effectively blocked the current induced by efficacious agonists (Ingram et al., 1997). Taken together, the results show that the number of active receptors appears to play a key role in the kinetics of MOR-activated conductance.

There is building evidence based on various fluorescence assays that G protein–coupled receptors, including MORs, exist in different states distinguished by the association with G proteins. Receptors preassociated with G proteins (precoupled receptors) are thought to signal more rapidly than receptors that are dependent on collision coupling (Nobles et al., 2005; Riven et al., 2006; Philip et al., 2007; reviewed in Lohse et al., 2008; Vilardaga 2010). The stability (and thus the relative number) of the precoupled receptors is reportedly very low for some receptors (α_2-adrenoceptor; Qin et al., 2008) and substantially greater for others (muscarininc M_3 receptor; Qin et al., 2011). Where functional studies have been done using the activation of GIRK-dependent currents, precoupling has been suggested (Zhang et al., 2002; Lober et al., 2006; Zhou et al., 2012). Those experiments examined receptors (including MOR) that were immobilized, and the mobility of G proteins, GIRK channels, or RGS proteins was assayed (Zhang et al., 2002; Lober et al., 2006; Zhou et al., 2012).

One possible explanation for the change in the rate of rise after MOR desensitization is that there is a small percentage of MORs that are in a state that favors rapid activation (precoupled). Photolysis of CYLE results in the rapid application of a high agonist concentration such that a large percentage of receptors are activated near simultaneously. This method is ideal for the detection of precoupled receptors. Even if the population of precoupled receptors is less than 20% of the total (Qin et al., 2008), these efficiently coupled receptors could be sufficient to effectively activate downstream effectors. Elimination of receptors through desensitization, antagonism with β-CNA, or acute dissociation of the cells may not change in the relative number of "precoupled" receptors, but the absolute number of these receptors may decrease to a level below the limit of detection. Thus, the rate of GIRK activation would be more dependent on the relatively large proportion of more slowly activated collision coupled receptors.

Acknowledgments

The author thanks Mathew Banghart, Luke D. Lavis, and Bernardo Sabatini for the generous gifts of CYLE and CNV-NLX; Mathew Banghart, Seksiri Arttamangkul, William Birdsong, and Erica Levitt for helpful discussion; and Shane Hentges and Chris Ford for comments on the manuscript.

Authorship Contributions

Participated in research design: Williams.
Conducted experiments: Williams.
Performed data analysis: Williams.
Wrote or contributed to the writing of the manuscript: Williams.

References

Banghart MR and Sabatini BL (2012) Photoactivatable neuropeptides for spatiotemporally precise delivery of opioids in neural tissue. *Neuron* **73**:249–259.

Banghart MR, Williams JT, Shah RC, Lavis LD, and Sabatini BL (2013) Caged naloxone reveals opioid signaling deactivation kinetics. *Mol Pharmacol* **84**: 687–695.

Birdsong WT, Arttamangkul S, Clark MJ, Cheng K, Rice KC, Traynor JR, and Williams JT (2013) Increased agonist affinity at the μ-opioid receptor induced by prolonged agonist exposure. *J Neurosci* **33**:4118–4127.

Fiorillo CD and Williams JT (1996) Opioid desensitization: interactions with G-protein-coupled receptors in the locus coeruleus. *J Neurosci* **16**:1479–1485.

Ingram S, Wilding TJ, McCleskey EW, and Williams JT (1997) Efficacy and kinetics of opioid action on acutely dissociated neurons. *Mol Pharmacol* **52**:136–143.

Just S, Illing S, Trester-Zedlitz M, Lau EK, Kotowski SJ, Miess E, Mann A, Doll C, Trinidad JC, and Burlingame AL et al. (2013) Differentiation of opioid drug effects by hierarchical multi-site phosphorylation. *Mol Pharmacol* **83**:633–639.

Lau EK, Trester-Zedlitz M, Trinidad JC, Kotowski SJ, Krutchinsky AN, and Burlingame AL, von Zastrow M. (2011) Quantitative encoding of the effect of a partial agonist on individual opioid receptors by multisite phosphorylation and threshold detection. *Cell Signal* **4**:ra52.

Levitt ES and Williams JT (2012) Morphine desensitization and cellular tolerance are distinguished in rat locus ceruleus neurons. *Mol Pharmacol* **82**:983–992.

Llorente J, Lowe JD, Sanderson HS, Tsisanova E, Kelly E, Henderson G, and Bailey CP (2012) μ-Opioid receptor desensitization: homologous or heterologous? *Eur J Neurosci* **36**:3636–3642.

Lober RM, Pereira MA, and Lambert NA (2006) Rapid activation of inwardly rectifying potassium channels by immobile G-protein-coupled receptors. *J Neurosci* **26**: 12602–12608.

Lohse MJ, Hein P, Hoffmann C, Nikolaev VO, Vilardaga JP, and Bünemann M (2008) Kinetics of G-protein-coupled receptor signals in intact cells. *Br J Pharmacol* **153** (Suppl 1):S125–S132.

Nobles M, Benians A, and Tinker A (2005) Heterotrimeric G proteins precouple with G protein-coupled receptors in living cells. *Proc Natl Acad Sci USA* **102**: 18706–18711.

Osborne PB and Williams JT (1995) Characterization of acute homologous desensitization of mu-opioid receptor-induced currents in locus coeruleus neurones. *Br J Pharmacol* **115**:925–932.

Philip F, Sengupta P, and Scarlata S (2007) Signaling through a G Protein-coupled receptor and its corresponding G protein follows a stoichiometrically limited model. *J Biol Chem* **282**:19203–19216.

Qin K, Dong C, Wu G, and Lambert NA (2011) Inactive-state preassembly of G(q)-coupled receptors and G(q) heterotrimers. *Nat Chem Biol* **7**:740–747.

Qin K, Sethi PR, and Lambert NA (2008) Abundance and stability of complexes containing inactive G protein-coupled receptors and G proteins. *FASEB J* **22**: 2920–2927.

Quillinan N, Lau EK, Virk M, von Zastrow M, and Williams JT (2011) Recovery from mu-opioid receptor desensitization after chronic treatment with morphine and methadone. *J Neurosci* **31**:4434–4443.

Riven I, Iwanir S, and Reuveny E (2006) GIRK channel activation involves a local rearrangement of a preformed G protein channel complex. *Neuron* **51**:561–573.

Scheibe SD, Bennett DB, Spain JW, Roth BL, and Coscia CJ (1984) Kinetic evidence for differential agonist and antagonist binding to bovine hippocampal synaptic membrane opioid receptors. *J Biol Chem* **259**:13298–13303.

Vilardaga J-P (2010) Theme and variations on kinetics of GPCR activation/deactivation. *J Recept Signal Transduct Res* **30**:304–312.

Virk MS, Arttamangkul S, Birdsong WT, and Williams JT (2009) Buprenorphine is a weak partial agonist that inhibits opioid receptor desensitization. *J Neurosci* **29**: 7341–7348.

Wang H-L, Chang W-T, Hsu C-Y, Huang P-C, Chow Y-W, and Li AH (2002) Identification of two C-terminal amino acids, Ser(355) and Thr(357), required for short-term homologous desensitization of mu-opioid receptors. *Biochem Pharmacol* **64**: 257–266.

Werling LL, Puttfarcken PS, and Cox BM (1988) Multiple agonist-affinity states of opioid receptors: regulation of binding by guanyl nucleotides in guinea pig cortical, NG108-15, and 7315c cell membranes. *Mol Pharmacol* **33**:423–431.

Williams JT, Ingram SL, Henderson G, Chavkin C, von Zastrow M, Schulz S, Koch T, Evans CJ, and Christie MJ (2013) Regulation of μ-opioid receptors: desensitization, phosphorylation, internalization, and tolerance. *Pharmacol Rev* **65**: 223–254.

Williams JT and North RA (1984) Opiate-receptor interactions on single locus coeruleus neurones. *Mol Pharmacol* **26**:489–497.

Zhang Q, Pacheco MA, and Doupnik CA (2002) Gating properties of GIRK channels activated by Galpha(o)- and Galpha(i)-coupled muscarinic m2 receptors in Xenopus oocytes: the role of receptor precoupling in RGS modulation. *J Physiol* **545**: 355–373.

Zhou H, Chisari M, Raehal KM, Kaltenbronn KM, Bohn LM, Mennerick SJ, and Blumer KJ (2012) GIRK channel modulation by assembly with allosterically regulated RGS proteins. *Proc Natl Acad Sci USA* **109**:19977–19982.

Address correspondence to: John T. Williams, Vollum Institute, Oregon Health & Science University, Portland, OR 97239. E-mail: williamj@ohsu.edu